Eur. Phys. J. B **15**, 193–197 (2000)

THE EUROPEAN PHYSICAL JOURNAL B

EDP Sciences

Novel mechanism for discrete scale invariance in sandpile models

M.W. Lee[1] and D. Sornette[1,2,3,a]

[1] Institute of Geophysics and Planetary Physics, University of California, Los Angeles, California 90095, USA
[2] Department of Earth and Space Science, University of California, Los Angeles, California 90095, USA
[3] LPMC[b] and Université de Nice-Sophia Antipolis, BP 71, Parc Valrose, 06108 Nice Cedex 2, France

Received 24 November 1999

Abstract. Numerical simulations and a mean-field analysis of a sandpile model of earthquake aftershocks in 1d, 2d and 3d Euclidean lattices determine that the average stress decays in a punctuated fashion after a main shock, with events occurring at characteristic times increasing as a geometrical series with a well-defined multiplicative factor which is a function of the stress corrosion exponent, the stress drop ratio and the degree of dissipation. These results are independent of the discrete nature of the lattice and stem from the interplay between the threshold dynamics and the power law stress relaxation. This novel mechanism of log-periodicity does not rely on a pre-existing discrete structural hierarchy of faults but is dynamical and reflects the existence of an approximately fixed stress drop together with the scale-free stress corrosion power law acting during inter-seismic phases.

PACS. 02.50.Ey Stochastic processes – 64.60.Ht Dynamic critical phenomena – 91.30.Px Phenomena related to earthquake prediction

Discrete scale invariance (DSI) [1] is the partial breaking of continuous scale invariance [2] in which a system or an observable is invariant only under scaling ratios that are integer powers of a fundamental factor λ. DSI leads to complex critical exponents (or dimensions), *i.e.* to log-periodic corrections to scaling, which reflect the existence of a discrete self-similar spectrum of characteristic scales decorating the usual scale-free power law behavior.

Several mechanisms responsible for this partial breaking of the continuous scale symmetry have been expounded, which include build-in pre-existing hierarchy [3], intermittent diffusion in discrete Euclidean lattices [4] and cascades of ultra-violet instabilities in growth processes and rupture [5]. Other situations are less well understood but can be traced back to special technical properties such as the non-unitary structure of the underlying field theory describing the coarse-grained properties of animals [6] and of quenched disordered spin systems with long-range interactions [7]. Another example is the gravitational collapse leading to critical black hole formation described by a system of partial differential equations possessing an asymptotic solution which can be understood from a renormalization group with a limit cycle having a single unstable mode [8].

Here, we present a novel scenario for DSI based on the interplay between the threshold dynamics characteristic of sandpile models and a scale-free relaxation process [9]. Specifically, we study a conceptual sandpile model [10] of earthquake aftershocks on a Euclidean discrete d-dimensional cubic lattice with L^d cells and periodic boundary conditions with $d = 1, 2, 3$. Our use of periodic boundary and our claim that our results are independent of the boundary conditions may seem surprising since it is well-known [11] that the stationary state of the "loading phase" depends strongly on the boundary conditions, *e.g.* for open boundary conditions, the stationary state is in a self-organised critical state, whereas this is not the case for a periodic boundary condition. The upshot is that the discrete scale invariance and associated log-periodic behavior that we document below are independent of the initial loading and of the nature of boundary conditions, making our results actually independent to any presence of self-organized criticality. Due to the nature of the relaxation process and of the stress transfer, the relaxation rates are modified significantly only at the edges of a ruptured region. This local process lessens the difference between open and closed boundary conditions. Our use of periodic boundary conditions in most of our simulations is performed in order to bring our system faster to the "thermodynamic limit" (finite-size effects are smaller) than in models using open boundary conditions.

The system is assumed to be paved of "elementary" faults, one in each cell. An elementary fault is the minimum fault element activated during an event. Each cell represents a region which is unloaded when an elementary fault is activated. We neglect the tensorial nature of the stress field and consider an anti-plane driving

[a] e-mail: sornette@naxos.unice.fr
[b] UMR 6622 du CNRS

configuration (anti-plane is also called mode III corresponding to a stress field having only two non-vanishing stress components σ_{xy} and σ_{yz}) in which loading and rupture are controlled by a single shear (vertical) force component $V(\mathbf{x})$ (recall that mode I is crack opening in tension, mode II is crack shearing along the long axis of the crack and mode III is crack shearing perpendicular to it [12]).

There are two distinct temporal phases. First, the stress is uniformly increased at a very slow rate on all cells to mimic the tectonic loading. Due to the rupture and loading rules described below, the system self-organises into a statistical stationary state, characterised by a power law distribution of event sizes [9,10]. Once this statistical stationarity state is established, we freeze the loading and the aftershock sequence starts, mimicking the aftermath of a great earthquake. The second phase is characterised by the fact that the aftershocks are not driven by the tectonic loading but by relaxation processes as described below. We obtain similar results without the initial loading phase. Thus our results are not dependent on the presence or absence of self-organized criticality typically associated with loading phases such as this.

An initial stress threshold $B(\mathbf{x})$ is assigned to each cell from a random uniform distribution in the interval $B_0[1-r, 1+r]$. We find similar results both for the annealed and quenched version of the model, in which either the thresholds are fixed or are resampled in the interval after each rupture. When the stress $V(\mathbf{x})$ in a cell at $\mathbf{x}$ becomes larger or equal to $B(\mathbf{x})$, the stress is re-distributed according to the rules

$$V(\mathbf{x})|^{\text{after}} = V(\mathbf{x})|^{\text{before}}(1-\gamma), \tag{1}$$

$$V(\mathbf{x})|^{\text{after}}_{\text{nn}} = V(\mathbf{x})|^{\text{before}}_{\text{nn}} + V(\mathbf{x})|^{\text{before}} \frac{(1-\beta)\gamma}{2d}. \tag{2}$$

Rule (2) applies to each of the 2d nearest neighbours (n.n.) of $\mathbf{x}$ carrying an initial stress $V(\mathbf{x})|^{\text{before}}_{\text{nn}}$ which evolves into $V(\mathbf{x})|^{\text{after}}_{\text{nn}}$. Because the toppling criterion (1) depends only on V and not on its gradient, the order of site toppling commute [13] but only in the case $\beta = 0$.

γ is the relative stress drop, with $\gamma = 1$ corresponding to a complete stress drop. β is the dissipation where $1-\beta$ quantifies the amount of stress drop transfered to n.n. and is known as the seismic efficiency. For $\gamma = 1$, (1, 2) are identical to the rules used in the non-conservative sandpile model [14], motivated from the coupling of blocks to a rigid upper driving plate in the Burridge-Knopoff model. Here, the dissipation accounts for the loss of stress and of stored elastic energy due to an earthquake under constant displacement conditions at the boundaries [15].

In the second relaxation phase, the loading stops and the thresholds decay in time according to the law

$$B(\mathbf{x}, t) = B(\mathbf{x}, t_0) - \frac{[V(\mathbf{x}, t)]^{\alpha}}{B(\mathbf{x}, t_0)} (t - t_0). \tag{3}$$

This model incorporates the mechanism of sub-critical crack growth and stress corrosion [16], which has been proposed as a possible delay mechanism for aftershocks [9,17,18]. The above form was derived from the equations of sub-critical crack growth as part of a complete model of aftershocks presented elsewhere [9]. In the absence of loading, events are triggered each time the thresholds decay below the local stresses. When this occurs, the stress redistribution obeys (1, 2). The system eventually relaxes after an infinite time and in an intermittent manner to an equilibrium of zero stress on all elements of the lattice. Contrary to the results of sandpile models [11], a closed conservative spring-block system has also been found to relax in a infinite time and in an intermittent manner to the zero-stress equilibrium with self-organized critical behavior [20]. It is this complex relaxation that we study. It occurs *via* the triggering of what can be called aftershocks which exhibit remarkable properties. The results presented below are also found for a version of the model with continuous elasticity [9,21] derived from reference [19] and are probably robust features of the general interplay between threshold dynamics and relaxation phenomena.

We have checked that our results are robust with respect to the choice of the power law relaxation rate (3): if one slightly changes the functional form for the stress relaxation, one still obtain an approximate Omori's law with log-periodicity and discrete scale invariance. There will however be higher order corrections, *i.e.* log-periodicity will come with several harmonics of decreasing amplitudes. We stress that the main message is not Omori's power law relaxation but the fact that there is a spontaneous breaking of the continuous scale invariance symmetry into a discrete scale invariance due to the interplay with the threshold dynamics.

We show here mostly the simulations for 2d systems of 20×20 elements (simulations have been performed with size up to 100×100 with no change of results) and in the annealed case where, after each toppling, thresholds are reassigned from the uniform distribution $B_0[1-r, 1+r]$ with $r = 0.75$. The system is up-dated by finding the site closest to rupture and incrementing time, so that this site reaches its threshold. Once a site becomes unstable due to either loading (in the first phase) or by the decay of the threshold (in the second phase), stress is distributed to n.n. according to (1, 2). The n.n. may also become unstable, releasing their stress and the process continues until no further nodes are unstable, thus defining an event. During the rupture process, time is "freezed" to ensure a separation of time scales between rupture (fast) and loading/decay (slow). When no further sites are unstable, loading or decay is continued until the next event, when time "freezes" again. Typically 3×10^3 to 15×10^3 events were sampled in the decay regime. The results are robust with respect to heterogeneity level r, open or closed boundary conditions, and to the size and dimension $d = 1, 2, 3$ of the lattice.

Figure 1 shows the rate of aftershocks $n(t)$ as a function of time after the loading has ceased. The $1/t$ decay is in full agreement with Omori's law for real aftershock sequences [22] and is very robust over a wide range of parameters, *i.e.* $\alpha > 0$, $\gamma > 0$ and $\beta < 1$. Typical values for the earth are $10 \leq \alpha \leq 100$, $\gamma \approx 5{-}15\%$ (stress drop) and $\beta \approx 99\%$ (corresponding to a seismic efficiency of

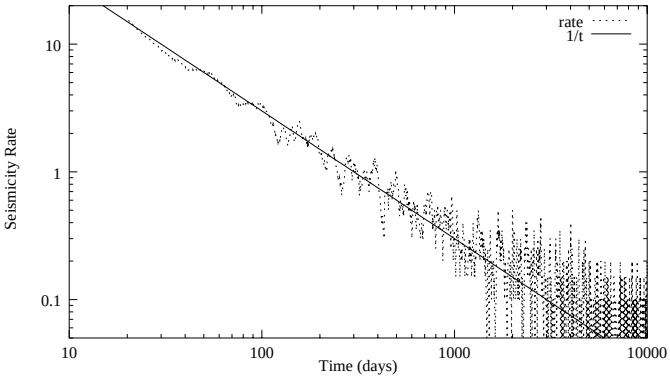

Fig. 1. Power law decay of the rate of aftershocks for a lattice of size 20×20 with $\alpha = 1$, $\gamma = 1$ and $\beta = 0.5$. The solid line is t^{-1}.

1%). The distribution of event sizes also follows a power law (Gutenberg-Richter for aftershocks), but in contrast to Omori's law, the exponent continuously depends on the three parameters. Furthermore, for large dissipation β, the power law extends only up to a maximum scale which decreases as $\beta \to 1$. This feature has also been observed for real earthquakes where the biggest characteristic earthquakes are thought to belong to a different class [23].

These results can be rationalized by the following mean field theory. From (3), we see that the time Δt needed for an isolated element to reach rupture is such that the threshold $B(\mathbf{x}, t_0 + \Delta t)$ decreases to the stress level $V(\mathbf{x})$. The mean field argument simply assumes that we can extend this result over all elements of the lattice by replacing $V(\mathbf{x})$ by the average stress $\langle V(t)\rangle_{\mathbf{x}}$ accounting for the influence of the possible loading by n.n. This approximation becomes better and better as the dissipation β increases and the dynamics of n.n. elements becomes increasingly uncoupled. This corresponds to a decreasing dependence on spatial inhomogeneities, which is exactly the underlying assumption of any mean-field approximation. We get

$$\Delta t \approx B_0^2 / \langle V\rangle_{\mathbf{x}}^{\alpha}, \tag{4}$$

where we have approximated $B_0 - \langle V\rangle_{\mathbf{x}}$ by B_0, since for large times the mean stress level becomes very low compared to the thresholds that are healed back to a typical value in the interval $B_0[1-r, 1+r]$ after each event. Expression (4) has the same form as obtained from a model of cracks undergoing sub-critical crack growth [9]. Over such a time interval, essentially one main event occurs on each site and, as a consequence, the average stress goes from $\langle V\rangle_{\mathbf{x}}$ to $(1-\gamma)\langle V\rangle_{\mathbf{x}}$, corresponding to a typical stress decrease $\gamma\langle V\rangle$. We can thus write

$$\frac{\mathrm{d}\langle V\rangle_{\mathbf{x}}}{\mathrm{d}t} \sim -\frac{\gamma\langle V\rangle_{\mathbf{x}}}{\Delta t} \approx -\frac{\gamma}{B_0^2}\ \langle V\rangle_{\mathbf{x}}^{1+\alpha}, \tag{5}$$

whose solution is

$$\langle V(t)\rangle_{\mathbf{x}} = (B_0^2/\alpha\gamma)^{1/\alpha}(t+c)^{-1/\alpha}. \tag{6}$$

c is a constant determined from the initial value of the average stress at the beginning of the aftershock relaxation sequence.

To get Omori's law, we recognise that the rate $n(t)$ of aftershocks is simply proportional to the rate with which the thresholds $B(\mathbf{x}, t)$ reach the stress level. $n(t)$ is also proportional to $1/\Delta t$. This yields

$$n(t) \propto \frac{\mathrm{d}B(\mathbf{x},t)}{\mathrm{d}t} \sim [V(\mathbf{x},t)]^{\alpha} \sim [\langle V(t)\rangle_{\mathbf{x}}]^{\alpha} \sim \frac{1}{(t+c)^{p}}, \quad \text{with } p = 1. \tag{7}$$

According to this mean field theory, Omori's law is obtained with the universal exponent $p = 1$ independently of the value of the stress-corrosion exponent α, as long as it is positive. For $\alpha = 0$, the average stress level decays exponentially fast with time and the rate of aftershocks is constant.

The mean field theory also provides a prediction of log-periodicity. The stress redistribution laws (1, 2) imply that, over a typical time Δt given by (4), the average stress undergoes the change $\langle V\rangle_{\mathbf{x}} \to \langle V\rangle_{\mathbf{x}}/\mu$, where

$$1/\mu = [f(d)(1-\gamma) + n_{\mathrm{eff}}\gamma(1-\beta)]/f(d). \tag{8}$$

$f(d)$ is a geometric factor counting the effective number of n.n. ($f(d) = 2d$ in the large dissipation limit $\beta \to 1$). The first contribution $(1-\gamma)$ in the r.h.s. of (8) is simply the initial stress minus the stress drop. The second contribution $n_{\mathrm{eff}}\gamma(1-\beta)/f(d)$ results from the number $n_{\mathrm{eff}} \sim 1$ of stress loading on a given element due to the earthquakes occurring on its neighbours.

Each time the average stress is decreased by a factor μ, we see from (4) that the time interval Δt is increased by a factor

$$\lambda = \mu^{\alpha}. \tag{9}$$

Since $\mu > 1$, the total time is essentially dominated by the last time interval between the two last cycles. This allows us to write an approximate scaling relation on the average stress $\langle V\rangle$:

$$\langle V(t)\rangle_{\mathbf{x}} = \mu\,\langle V(\lambda t)\rangle_{\mathbf{x}}. \tag{10}$$

Since the aftershock rate $n(t)$ is proportional to $\langle V\rangle_{\mathbf{x}}^{\alpha}$, this leads to

$$n(t) = \lambda n(\lambda t), \tag{11}$$

using (9). Looking for a power law solution $n(t) \sim t^{-p}$, we retrieve Omori's exponent $p = 1$. A more general solution is the power law t^{-1} multiplied by a periodic function of $\ln t$,

$$n(t) = t^{-1} P_1(\ln t/\ln\lambda), \tag{12}$$

where $P_1(x)$ is periodic with period one. Expanding this periodic function into its Fourier series gives

$$n(t) = t^{-1}\sum_{k=-\infty}^{+\infty} a_k t^{\mathrm{i}2\pi k/ln\lambda}, \tag{13}$$

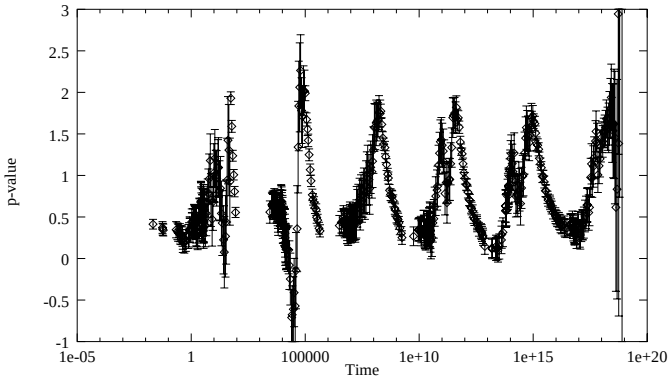

Fig. 2. Local exponent $p(t)$ for $\alpha = 1, \gamma = 1, \beta = 0.999$. The window size is 100 events.

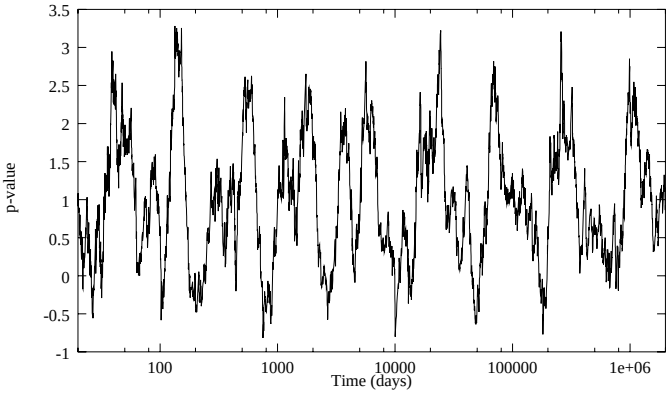

Fig. 3. p-value as a function of time for the case of $\alpha = 25$, $\gamma = 0.05$, $\beta = 0.99$. The window size is 150 events.

with $a_{-k} = a_k$, which defines the discrete spectrum of complex exponents $p_k = 1 - \mathrm{i}\frac{2\pi k}{\ln \lambda}$. The leading correction to the power Omori's law gives the log-periodic expression

$$n\,(t) = \frac{1}{t}\left(a_0 + a_1 \cos\left(2\pi \frac{\ln t}{\ln \lambda}\right)\right). \tag{14}$$

To test this prediction, we find that the local exponent $p(t)$, defined by $\mathrm{d}\ln n\,(t)\,/\mathrm{d}\ln t = -p\,(t)$, gives the most sensitive measure of deviation from the $1/t$ Omori's law. We estimate $p(t)$ by a maximum likelihood estimator in a running window ending at t [9]. Defining the starting t and ending t_{U} times of a window and the average $\langle \ln t_i \rangle$ of the logarithms of all N aftershock times within this window, the MLE is

$$p(t) \approx 12 \frac{\ln \sqrt{t t_{\mathrm{U}}} - \langle \ln t_i \rangle)}{(\ln(t_{\mathrm{U}}/t))^2 + 1}, \tag{15}$$

with a variance

$$\sigma^2 \approx 12\,(N-1)^{-1}\,(\ln(t_{\mathrm{U}}/t))^{-2}. \tag{16}$$

The estimation of $p(t)$ is very robust over a large set of window sizes and have been tested thoroughly on synthetic Omori's laws [24].

Figure 2 shows the local exponent $p\,(t)$ as a function of time t estimated using a window size of 100 events. Clear log-periodic oscillations around $p \approx 1$ can be identified with a (log-)frequency of ≈ 0.12 giving a preferred scale factor $\lambda \approx 3500$ in reasonable agreement with the theoretical value of 4000 calculated from (8, 9). Increasing the window size with t or keeping a window with size fixed in time provides the same estimate.

Figure 3 presents $p(t)$ for the stress corrosion exponent $\alpha \approx 25$, a value estimated from a set of adjacent time-delayed multiple events in western Japan [18], for a stress drop $\gamma = 5\%$ and a seismic efficiency of 1%, *i.e.* $\beta = 0.99$. The measured scaling factor is now $\lambda = 3.5$ while the mean field prediction is $\lambda = 3.6$.

The comparisons between the numerical simulations and the predictions of the mean field theory are presented in Figures 4–6. The mean field theory, while not perfect, accounts well for most of the behavior. Results for a lattice size of 50×50 are added in Figure 4 to illustrate the

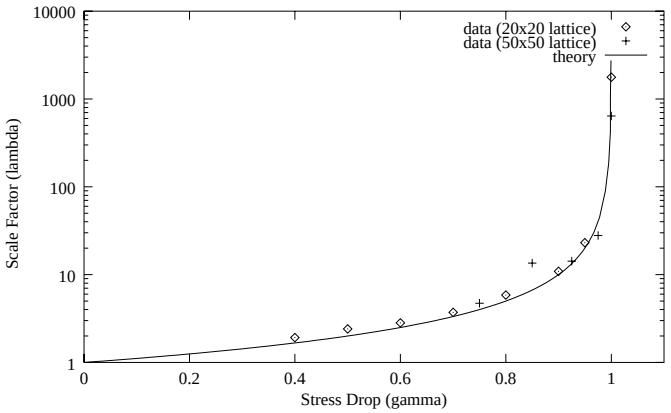

Fig. 4. Scaling factor λ as a function of stress drop γ for $\beta = 0.999$ and $\alpha = 1$.

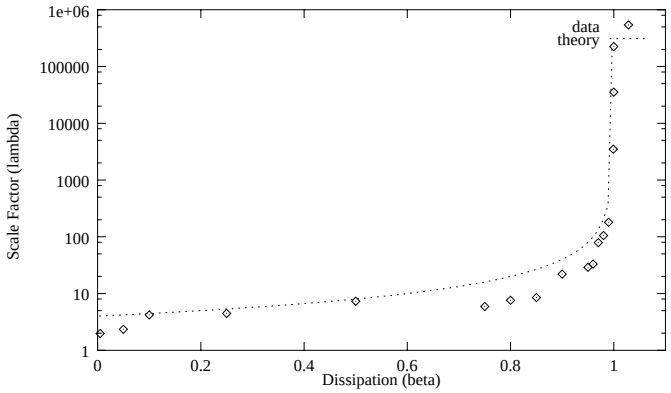

Fig. 5. Scaling factor λ as a function of β for $\alpha = 1$ and $\gamma = 1$.

independence on lattice size. Other simulations have been performed with sizes up to 100×100 with the same results. We also have checked that λ depends on the space dimension d for $d = 1, 2, 3$ as predicted from (8, 9).

Discrete scale invariance and its log-periodic signature is associated in this model with the threshold nature of the dynamics. The discrete scaling emerges from the fact that the thresholds are healed back to a value close to B_0 after each rupture and then have to decay down to the current stress threshold to trigger the next rupture. When

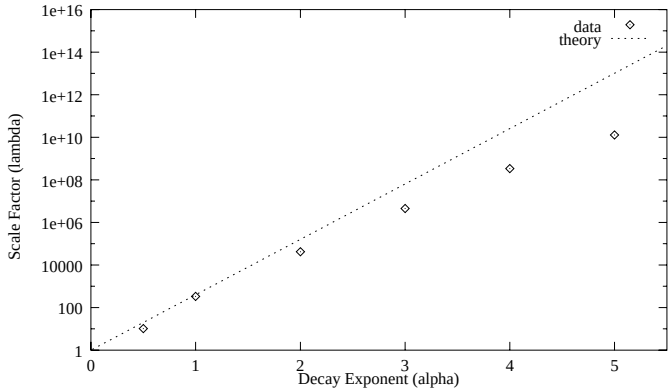

Fig. 6. Scaling factor λ as a function of α for $\beta = 0.99$ and $\gamma = 1$.

this occurs, the stress jumps to a smaller value by a finite amount and can also later be reloaded again by active neighbours. It is fundamentally these *finite* jumps in the stress proportional to the current stress (which are thus scale-free) which are at the origin of discrete scale invariance and log-periodicity. This novel mechanism of log-periodicity does not rely on a pre-existing discrete structural hierarchy of faults but is dynamical and reflects the existence of an approximately fixed stress drop together with the scale-free stress corrosion power law acting during inter-seismic phases.

This study suggests to search for log-periodic signatures in real aftershock sequences, with the potential bonus that log-periodicity would constrain the stress drop ratio, an elusive quantity to estimate by direct seismic measurements. A systematic analysis on more than thirty large aftershock sequences found log-periodicity [9] but was unable to conclude decisively on the mechanism producing this log-periodicity [24], due to a noise level which is comparable to the amplitude of the signal. Further studies are thus called for.

We are especially grateful to A. Johansen and L. Knopoff for very stimulating discussions. M.L. thanks the Physics department at UCLA for hospitality.

References

1. D. Sornette, Phys. Rep. **297**, 239 (1998).
2. *Scale invariance and beyond*, edited by B. Dubrulle, F. Graner, D. Sornette (EDP Sciences, les Ulis, and Springer, Berlin, 1997).
3. B. Derrida, L. De Seze, C. Itzykson, J. Stat. Phys. **33**, 559 (1983); B. Derrida, C. Itzykson, J.M. Luck, Commun. Math. Phys. **94**, 115 (1984).
4. J. Bernasconi, W.R. Schneider, J. Phys. A **15**, L729 (1983); D. Stauffer, D. Sornette, Physica A **252**, 271 (1998).
5. D. Sornette, A. Johansen, A. Arnéodo, J.-F. Muzy, H. Saleur, Phys. Rev. Lett. **76**, 251 (1996); Y. Huang, G. Ouillon, H. Saleur, D. Sornette, Phys. Rev. E **55**, 6433 (1997); A. Johansen, D. Sornette, Int. J. Mod. Phys. C **9**, 433 (1998).
6. H. Saleur, D. Sornette, J. Phys. I France **6**, 327 (1996).
7. A. Aharony, Phys. Rev. B **12**, 1049 (1975); J.-H. Chen, T.C. Lubensky, Phys. Rev. B **16**, 2106 (1977); D.E. Khmelnitskii, Phys. Lett. A **67**, 59 (1978); Phys. Rev. B **26**, 154-170 (1982); A. Weinrib, B.I. Halperin, Phys. Rev. B **27**, 413 (1983).
8. M.W. Choptuik, Phys. Rev. Lett. **70**, 9 (1993); C. Gundlach, Phys. Rev. D **55**, 695 (1997).
9. M.W. Lee, *Unstable fault interactions and earthquake self-organization*, Ph.D. Thesis, UCLA (1999).
10. P. Bak, C. Tang, J. Geophys. Res. **94**, 15635 (1989); K. Ito, M. Matsuzaki, J. Geophys. Res. **95**, 6853 (1990).
11. P. Grassberger, Phys. Rev. E **49**, 2436 (1994).
12. H.J. Herrmann, S. Roux, *Statistical models for the fracture of disordered media* (North Holland, Amsterdam, 1990).
13. D. Dhar, Phys. Rev. Lett. **64**, 1613 (1990).
14. K. Christensen, Z. Olami, J. Geophys. Res. **97**, 8729 (1992).
15. Y. Huang, H. Saleur, C.G. Sammis, D. Sornette, Europhys. Lett. **41**, 43 (1998).
16. R.J. Charles, J. Appl. Phys. **29**, 1549 (1958); B.K. Atkinson, J. Geophys. Res. **89**, 4077 (1984).
17. C.H. Scholz, Seism. Soc. Am. Bull. **58**, 1117 (1968).
18. S. Das, C.H. Scholz, J. Geophys. Res. **86**, 6039 (1981); B. Shaw, Geophys. Res. Lett. **20**, 907 (1993).
19. P. Cowie, C. Vanneste, D. Sornette, J. Geophys. Res. **98**, 21809 (1993); D. Sornette, P. Miltenberger, C. Vanneste, Pure Appl. Geophys. **142**, 491 (1994).
20. K.T. Leung, J.V. Andersen, D. Sornette, Phys. Rev. Lett. **80**, 1916 (1998); Physica A **254**, 85 (1998).
21. L. Knopoff, M.W. Lee, The self-organization of earthquake aftershocks (to be published).
22. F. Omori, J. Coll. Sci. Japan Imp. Univ. **7**, 111 (1895); T. Utsu, Geophys. Mag. **30**, 521 (1961).
23. C.H. Scholz, Bull. Seism. Soc. Am. **84**, 215 (1994); A. Sornette, D. Sornette, Bull. Seism. Soc. Am. **84**, 1679 (1994); C.H. Scholz, Bull. Seism. Soc. Am. **87**, 1074 (1997); *ibid.* **88**, 1325 (1998); J. Laherrere, D. Sornette, Eur. Phys. J. B **2**, 525 (1998).
24. Y. Huang, A. Johansen, M.W. Lee, H. Saleur, D. Sornette, Mechanisms for Log-Periodicity in Under-Sampled Data: Relevance for Earthquake Aftershocks, submitted to J. Geophys. Res.